Eur. Phys. J. C (2016) 76:419
DOI 10.1140/epjc/s10052-016-4270-y

THE EUROPEAN PHYSICAL JOURNAL C

Regular Article - Theoretical Physics

Predictions for squeezed back-to-back correlations of $\phi\phi$ and K^+K^- in high-energy heavy-ion collisions by event-by-event hydrodynamics

Yong Zhang[1], **Wei-Ning Zhang**[1,2,a]

[1] School of Physics and Optoelectronic Technology, Dalian University of Technology, Dalian 116024, Liaoning, China
[2] Department of Physics, Harbin Institute of Technology, Harbin 150006, Heilongjiang, China

Received: 12 October 2015 / Accepted: 15 July 2016 / Published online: 27 July 2016

Abstract We calculate the squeezed back-to-back correlation (BBC) functions of $\phi\phi$ and K^+K^- for heavy-ion collisions at RHIC and LHC energies, using $(2+1)$-dimensional hydrodynamics with fluctuating initial conditions. The BBC functions averaged over event-by-event calculations for many events for the hydrodynamic sources are smoothed as a function of the particle momentum. For heavy-ion collisions of Au + Au at $\sqrt{s_{NN}} = 200$ GeV, the BBC functions are larger than those for collisions of Pb + Pb at $\sqrt{s_{NN}} = 2.76$ TeV. The BBC of $\phi\phi$ may possibly be observed in peripheral collisions at the RHIC and LHC energies. It is large for the smaller sources of Cu + Cu collisions at $\sqrt{s_{NN}} = 200$ GeV.

1 Introduction

In the late 1990s, it was shown [1,2] that the mass modification of the particles in the hot and dense hadronic sources can lead to a squeezed back-to-back correlation (BBC) of boson–antiboson pairs in high-energy heavy-ion collisions. This BBC caused by the interactions in medium is different from the pure quantum statistical correlations between the bosons with different isospins [3,4], which are negligible in high-energy heavy-ion collisions because the Fourier transformation of the source density, $|\tilde{\rho}(\vec{0}, m)|$, is very small even for the lightest meson [2,5]. Since it is associated with the source medium, the investigations of the BBC possibly provide another way to understand the thermal and dynamical properties of the hadronic sources formed in high-energy heavy-ion collisions, in addition to particle yields and spectra.

[a] e-mail: wnzhang@dlut.edu.cn

The BBC function is defined as [1,2]

$$C(\mathbf{k}, -\mathbf{k}) = 1 + \frac{|G_s(\mathbf{k}, -\mathbf{k})|^2}{G_c(\mathbf{k}, \mathbf{k}) G_c(-\mathbf{k}, -\mathbf{k})}, \tag{1}$$

where $G_c(\mathbf{k}_1, \mathbf{k}_2)$ and $G_s(\mathbf{k}_1, \mathbf{k}_2)$ are the chaotic and squeezed amplitudes, respectively,

$$G_c(\mathbf{k}_1, \mathbf{k}_2) = \sqrt{\omega_{\mathbf{k}_1} \omega_{\mathbf{k}_2}}\, \langle a^\dagger_{\mathbf{k}_1} a_{\mathbf{k}_2} \rangle, \tag{2}$$
$$G_s(\mathbf{k}_1, \mathbf{k}_2) = \sqrt{\omega_{\mathbf{k}_1} \omega_{\mathbf{k}_2}}\, \langle a_{\mathbf{k}_1} a_{\mathbf{k}_2} \rangle, \tag{3}$$

where $a_{\mathbf{k}}$ and $a^\dagger_{\mathbf{k}}$ are the annihilation and creation operators of the free boson with momentum $\mathbf{k}$ and mass m, $\langle \cdots \rangle$ indicates the ensemble average. For a homogeneous source with volume V and temperature T, the BBC function can be written as [2]

$$C(\mathbf{k}, -\mathbf{k}) = 1 + \frac{V\, |c_{\mathbf{k}}\, s^*_{\mathbf{k}}\, n_{\mathbf{k}} + c_{-\mathbf{k}}\, s^*_{-\mathbf{k}}\, (n_{-\mathbf{k}} + 1)|^2}{V\, [n_1(\mathbf{k})\, n_1(-\mathbf{k})]}, \tag{4}$$

where $c_{\mathbf{k}}$ and $s_{\mathbf{k}}$ are the coefficients of the Bogoliubov transformation between the creation (annihilation) operators of the quasiparticle in medium with modified mass m_* and the free observed particle [1,2], $n_{\mathbf{k}}$ is the boson distribution,

$$n_{\mathbf{k}} = \frac{1}{\exp(\Omega_{\mathbf{k}}/T) - 1}, \quad \left(\Omega_{\mathbf{k}} = \sqrt{\mathbf{k}^2 + m_*^2}\right), \tag{5}$$

and

$$n_1(\mathbf{k}) = |c_{\mathbf{k}}|^2\, n_{\mathbf{k}} + |s_{-\mathbf{k}}|^2 (n_{-\mathbf{k}} + 1). \tag{6}$$

The BBC function $C(\mathbf{k}, -\mathbf{k})$ will be 1 if there is no mass modification. However, for a finite mass modification, $\delta m^2 = m^2 - m_*^2$, $f_{\mathbf{k}} \sim \delta m^2/(4\mathbf{k}^2)$ as $|\mathbf{k}| \to \infty$, and the BBC function will increase with increasing particle momentum [2], $C(\mathbf{k}, -\mathbf{k}) \sim 1 + 1/|s_{-\mathbf{k}}|^2 \sim 1 + \mathbf{k}^4/(\delta m^2/4)^2$.

For hydrodynamic sources, with the formula derived by Makhlin and Sinyukov [6,7], the chaotic and squeezed amplitudes can be expressed as [2,8–10]

$$G_c(\mathbf{k}_1,\mathbf{k}_2)=\int\frac{\mathrm{d}^4\sigma_\mu(r)}{(2\pi)^3}K^\mu_{1,2}\,e^{i\,q_{1,2}\cdot r}\Big\{|c'_{\mathbf{k}'_1,\mathbf{k}'_2}|^2\,n'_{\mathbf{k}'_1,\mathbf{k}'_2}+|s'_{-\mathbf{k}'_1,-\mathbf{k}'_2}|^2\,[\,n'_{-\mathbf{k}'_1,-\mathbf{k}'_2}+1]\Big\},\tag{7}$$

$$G_s(\mathbf{k}_1,\mathbf{k}_2)=\int\frac{d^4\sigma_\mu(r)}{(2\pi)^3}K^\mu_{1,2}\,e^{2i\,K_{1,2}\cdot r}\Big\{s'^*_{-\mathbf{k}'_1,\mathbf{k}'_2}c'_{\mathbf{k}'_2,-\mathbf{k}'_1}\times n'_{-\mathbf{k}'_1,\mathbf{k}'_2}+c'_{\mathbf{k}'_1,-\mathbf{k}'_2}s'^*_{-\mathbf{k}'_2,\mathbf{k}'_1}[n'_{\mathbf{k}'_1,-\mathbf{k}'_2}+1]\Big\}.\tag{8}$$

Here $\mathrm{d}^4\sigma_\mu(r)$ is the four-dimensional element of the freeze-out hypersurface, $q^\mu_{1,2}=k^\mu_1-k^\mu_2$, $K^\mu_{1,2}=(k^\mu_1+k^\mu_2)/2$, and $\mathbf{k}'_i$ is the local-frame momentum corresponding to $\mathbf{k}_i$ $(i=1,2)$. The local quantities, $c'_{\mathbf{k}'_1,\mathbf{k}'_2}$, $s'_{\mathbf{k}'_1,\mathbf{k}'_2}$, and $n'_{\mathbf{k}'_1,\mathbf{k}'_2}$ are the coefficients of the Bogoliubov transformation and boson distribution associated with the particle pair (see in Ref. [10]).

In Eq. (8), the factor $e^{2iK_{1,2}\cdot r}$ is equal to $e^{2i\omega_\mathbf{k}t}$ for $\mathbf{k}_1=\mathbf{k}$, $\mathbf{k}_2=-\mathbf{k}_1=-\mathbf{k}$. So the BBC function $C(\mathbf{k},-\mathbf{k})$ is sensitive to the temporal distribution of the freeze-out points [2,8–11]. Recent research [10] indicates that the BBC functions for the hydrodynamic sources with Gaussian initial-energy distributions exhibit oscillations as a function of the particle momentum because of the sharp falls of temporal freeze-out distributions at long times. Investigating the BBC behavior and predicting its effect in high-energy heavy-ion collisions based on more realistic models is of great interest [10]. In this work, we investigate the BBC functions for the hydrodynamic sources with event-by-event fluctuating initial conditions (FIC). We use (2 + 1)-dimensional hydrodynamics with the HIJING [12,13] FIC and the equation of state s95p-PCE [14] to describe the source evolution as in Ref. [15], and we investigate the BBC functions of $\phi\phi$ and K^+K^- for heavy-ion collisions of Au + Au at $\sqrt{s_{NN}}=200$ GeV at the Relativistic Heavy Ion Collider (RHIC) and Pb + Pb at $\sqrt{s_{NN}}=2.76$ TeV at the Large Hadron Collider (LHC), respectively. Our investigation indicates that the BBC functions averaged over event-by-event calculations for many events for the hydrodynamic sources with the FIC are smoothed and without the oscillations appearing in the BBC functions for the hydrodynamic sources with Gaussian initial-energy distributions [10]. For heavy-ion collisions at the RHIC and LHC energies, the BBC of $\phi\phi$ may possibly be observed in peripheral collisions. The investigations for the BBC functions of $\phi\phi$ for Cu + Cu collisions at $\sqrt{s_{NN}}=200$ GeV indicate that the BBC is large for smaller sources.

The rest of this paper is organized as follows. In Sect. 2, we give a brief review on the relativistic hydrodynamic model used in this work, and discuss the space-time distributions of particle freeze-out points for the hydrodynamic sources with the FIC. In Sect. 3, we present the BBC functions of $\phi\phi$ and K^+K^- for heavy-ion collisions of Au + Au and Pb + Pb at the RHIC and LHC energies, respectively. The dependences of the BBC functions on the azimuthal angle and pseudo-rapidity of the particles are also investigated in this section. In Sect. 4, we investigate the source space-time distributions and the BBC functions of ϕ meson for the smaller sources in Cu + Cu collisions at $\sqrt{s_{NN}}=200$ GeV. Finally, a summary and conclusions of this paper are given in Sect. 5.

2 (2 + 1)-Dimensional hydrodynamic sources

Relativistic hydrodynamics has been extensively applied in high-energy heavy-ion collisions. In this work, we use the ideal relativistic hydrodynamics in (2 + 1) dimensions to describe the transverse expansion of the particle-emitting sources formed in ultrarelativistic heavy-ion collisions, and we adopt the Bjorken boost-invariant hypothesis [16] for the longitudinal evolution of the sources. The hydrodynamic equations of motion for the sources with zero net baryon density are from the local conservation of energy-momentum [17,18]. Under the assumption of Bjorken longitudinal boost invariance, we need only to solve the transverse equations of motion in the $z=0$ plane [15], and the hydrodynamic solutions at $z\neq 0$ $(v^z=z/t)$ can be obtained by the longitudinal boost invariance [19,20].

Assuming the local equilibrium of system is reached at time τ_0, we construct the initial-energy density of the hydrodynamic source at $z=0$, by using the AMPT code [21] in which the HIJING is used for generating the initial conditions [20,22],

$$\epsilon(\tau_0,x,y;z=0)=K\sum_\alpha\frac{p_{\perp\alpha}}{\tau_0}\frac{1}{2\pi\sigma_0^2}\times\exp\left\{-\frac{[x-x_\alpha(\tau_0)]^2+[y-y_\alpha(\tau_0)]^2}{2\pi\sigma_0^2}\right\}.\tag{9}$$

Here $p_{\perp\alpha}$ is the transverse momentum of parton α in the fluid element at (x,y), $x_\alpha(\tau_0)$ and $y_\alpha(\tau_0)$ are the transverse coordinates of the parton at τ_0, σ_0 is a transverse width parameter, and K is a scale factor which can be adjusted to fit the experimental data of produced hadrons [22]. The initial velocity of the fluid element is then determined by the initial-energy density and the average transverse momentum of the partons in the element.

As in Ref. [15], we solve the hydrodynamic equations numerically by the HLLE scheme and the Sod operation splitting method [17,23–34]. In the calculations, we use the equation of state s95p-PCE [14], which combines the hadron resonance gas at low temperatures and the lattice QCD results at high temperatures, and take the parameters $\sigma_0=0.6$ fm, $\tau_0=0.6$ and 0.4 fm/c for the heavy-ion collisions at the RHIC and LHC, respectively. With these parameter values

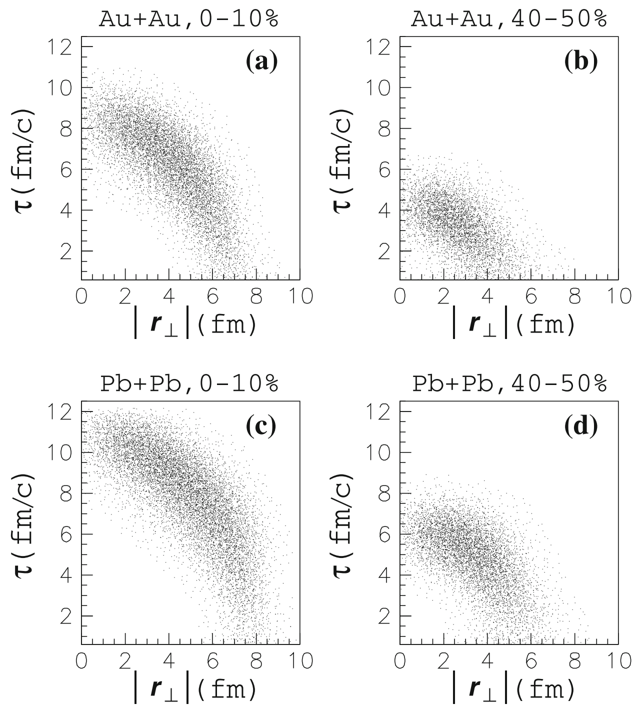

Fig. 1 Distributions of the freeze-out points of ϕ meson in the $z = 0$ plane for central and peripheral collisions of Au + Au at $\sqrt{s_{NN}} = 200$ GeV and Pb + Pb at $\sqrt{s_{NN}} = 2.76$ TeV, plotted with 2000 events

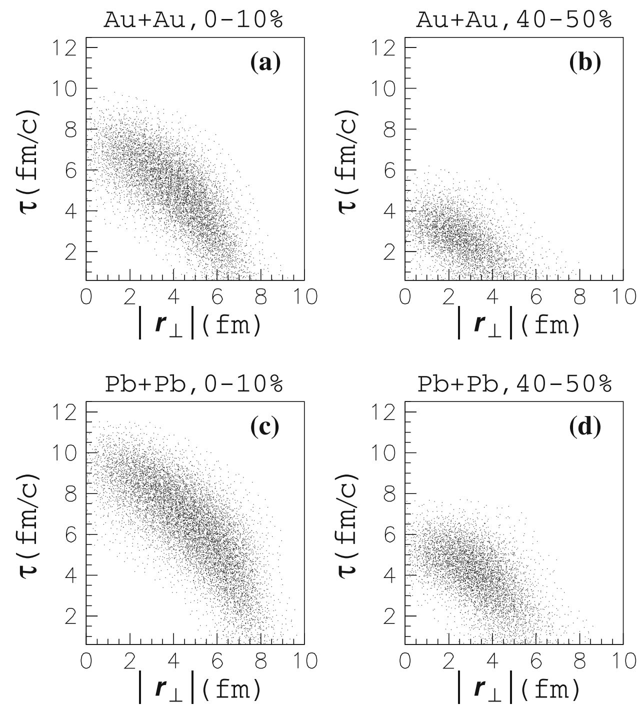

Fig. 2 Distributions of the freeze-out points of the K meson in the $z = 0$ plane for the central and peripheral collisions as in Fig. 1, plotted with 2000 events

the hydrodynamic results of transverse momentum spectra and elliptic flow of identical pion and charged hadrons are consistent with the experimental data at the RHIC and LHC [15,22].

For hydrodynamic sources with a Bjorken cylinder, the four-dimensional element of the freeze-out hypersurface can be written as

$$d^4\sigma_\mu(r) = f_\mu(\tau, \mathbf{r}_\perp, \eta)\, d\tau d^2\mathbf{r}_\perp d\eta, \tag{10}$$

where τ, $\mathbf{r}_\perp$, and η are the proper time, transverse coordinate, and space-time rapidity of the element. The function $f_\mu(\tau, \mathbf{r}_\perp, \eta)$ is related to the freeze-out mechanism that is considered, and $K^\mu_{1,2} f_\mu(\tau, \mathbf{r}_\perp, \eta)$ corresponds to the source distributions of proper time and space in the calculations [see Eqs. (7) and (8)]. In this work we assume that ϕ and K mesons are frozen out at fixed temperatures $T_f = 140$ and 160 MeV, respectively, and we use the AZHYDRO technique [18,35,36] to calculate the freeze-out hypersurface element.

We plot in Fig. 1 the space-time distributions of the freeze-out points, $k^\mu f_\mu(\tau, \mathbf{r}_\perp, \eta)$, of ϕ meson in the $z = 0$ plane for central and peripheral heavy-ion collisions of Au + Au at $\sqrt{s_{NN}} = 200$ GeV at the RHIC and Pb + Pb at $\sqrt{s_{NN}} = 2.76$ TeV at the LHC. Here, the event number for both the RHIC and the LHC collisions is 2000. The regions of impact parameter b for the chosen centralities 0–10 and 40–50 % are taken to be 0–4.2 and 9.0–10.2 fm [37], respectively. One can see that the width of the distributions increases with decreasing collision centrality and increasing collision energy. For the hydrodynamic sources with FIC, the freeze-out distributions are more dispersive compared to the hydrodynamic sources with the Gaussian initial conditions [10]. In Fig. 2, we plot the space-time distributions of the freeze-out points of the K meson in the $z = 0$ plane for the central and peripheral collisions as in Fig. 1. The widths of the freeze-out distributions of K meson are smaller than those of the ϕ meson because of the higher freeze-out temperature of the K meson.

In Fig. 3, we show the normalized distributions of time and transverse coordinate of ϕ freeze-out points in the $z = 0$ plane for different single events (thin dashed lines) and 2000 events (thick solid lines), for heavy-ion collisions of Au + Au and Pb + Pb at the RHIC and LHC energies, respectively. One can see that the distributions for single events are fluctuated and these fluctuations are smoothed in the distributions for 2000 events.

3 BBC functions for Au + Au at RHIC and Pb + Pb at LHC

Because of the fluctuations of the space-time coordinates of freeze-out points, the BBC functions for single events are fluctuated. However, these fluctuations can be smoothed in the BBC functions averaged over event-by-event calculations for many events,

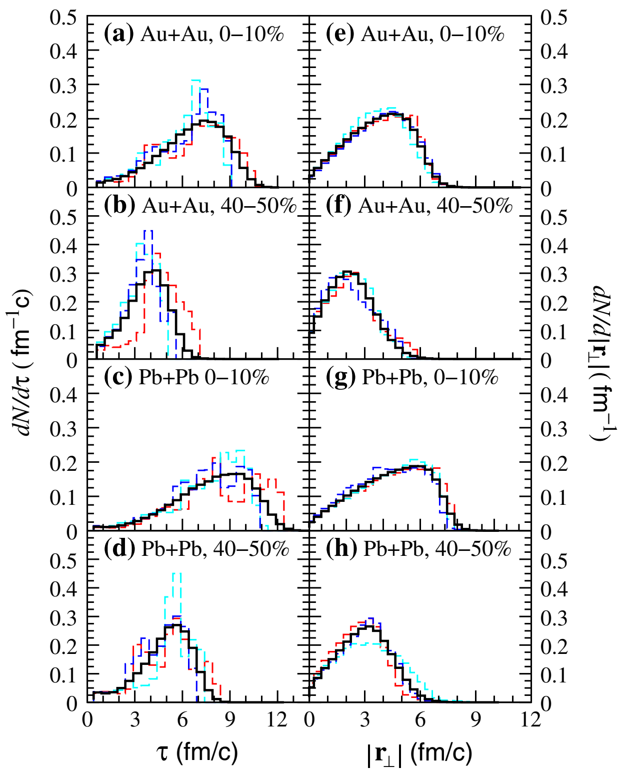

Fig. 3 Normalized distributions of time and transverse coordinate of the ϕ freeze-out points in the $z = 0$ plane for the heavy-ion collisions as in Fig. 1. The *thin dashed lines* are for different single events and the *thick solid lines* are for 2000 events

$$C(\mathbf{k}, -\mathbf{k}) = \frac{\frac{1}{N_E}\sum_{i=1}^{N_E}\left[G_{ci}(\mathbf{k},\mathbf{k})G_{ci}(-\mathbf{k},-\mathbf{k}) + |G_{si}(\mathbf{k},-\mathbf{k})|^2\right]}{\frac{1}{N_E}\sum_{i=1}^{N_E} G_{ci}(\mathbf{k},\mathbf{k})G_{ci}(-\mathbf{k},-\mathbf{k})}, \tag{11}$$

where N_E is the total event number.

We show in Fig. 4 the BBC functions of $\phi\phi$ averaged over event-by-event calculations for central and peripheral collisions of Au + Au at $\sqrt{s_{NN}} = 200$ GeV and Pb + Pb at $\sqrt{s_{NN}} = 2.76$ TeV. In the calculations of the BBC functions in this work, the total event number N_E for each kind of heavy-ion collision is 2000, and the space-time rapidity of source is taken to be $|\eta| \le 1$. Unlike the oscillations appearing in the BBC functions for the hydrodynamic sources with Gaussian distributions of initial-energy density [10], the BBC functions for the hydrodynamic sources with FIC vary smoothly with respect to the particle momentum. This is because the oscillations in the single-event BBC functions are canceled each other in the BBC functions averaged over event-by-event calculations for many events. From Fig. 4 one can see that the BBC functions for peripheral collisions are larger than those for central collisions. Also, it can be seen that the BBC functions for collisions at the RHIC energy are larger than those for collisions at the LHC energy.

In Eqs. (7) and (8), the factors $e^{iq_{1,2}\cdot r}$ and $e^{2iK_{1,2}\cdot r}$ are equal to 1 and $e^{2i\omega_{\mathbf{k}}t}$, respectively, for $\mathbf{k}_1 = \mathbf{k}$, $\mathbf{k}_2 = -\mathbf{k}_1 = -\mathbf{k}$. The BBC function $C(\mathbf{k}, -\mathbf{k})$ defined with Eq. (1) is proportional to the square of the Fourier transformation of the source temporal distribution with the weight $[s'^*_{-\mathbf{k}'_1,\mathbf{k}'_2} c'_{\mathbf{k}'_2,-\mathbf{k}'_1} n'_{-\mathbf{k}'_1,\mathbf{k}'_2} + c'_{\mathbf{k}'_1,-\mathbf{k}'_2} s'^*_{-\mathbf{k}'_2,\mathbf{k}'_1}(n'_{\mathbf{k}'_1,-\mathbf{k}'_2} + 1)]$, and the effects of the source spatial distribution in the numerator and denominator in Eq. (1) may cancel out partially. So, the values of the BBC function are mainly related to the source temporal distribution, particle mass, mass shift, and source temperature. Because we use the same freeze-out temperature for the ϕ meson in the calculations for the collisions with different centralities and energies, the main reason of the dependences of the ϕ BBC function on the collision centrality and energy (see Fig. 4 for fixed k and m_*) is that the temporal distribution of the source is narrower in peripheral collisions and becomes wider with increasing collision energy (see Fig. 1).

We show in Fig. 5 the BBC functions of K^+K^- averaged over event-by-event calculations for central and peripheral collisions of Au + Au at $\sqrt{s_{NN}} = 200$ GeV and Pb + Pb at $\sqrt{s_{NN}} = 2.76$ TeV. As compared to the results of the BBC functions of $\phi\phi$, the BBC functions of K^+K^- are much smaller. This is mainly because the higher freeze-out temperature and smaller mass of the K meson lead to larger values of $e^{-k^\mu u_\mu/T_f}$ in the calculations of BBC functions.

For anisotropic sources, the anisotropic source velocity may lead to the dependence of the BBC function on the direction of particle momentum [10,38]. We show in Fig. 6 the dependence of the average BBC functions of $\phi\phi$, $\langle C(\mathbf{k}, -\mathbf{k})\rangle_{|\mathbf{k}|}$, on the cosine of the particle azimuthal angle ψ for the collisions at the RHIC and LHC energies. Here, m_* is taken as 1.05 GeV, corresponding approximately to the middle between the valley and peak of the BBC function (see Fig. 4), and the momentum region averaged is 0–1 GeV/c. The BBC functions decrease with increasing cos ψ more rapidly for peripheral collisions because the source transverse velocities are more anisotropic in this case [10,38].

We show in Fig. 7 the dependence of the average BBC functions of $\phi\phi$, $\langle C(\mathbf{k}, -\mathbf{k})\rangle_{|\mathbf{k}|}$, on the particle pseudorapidity for the collisions at the RHIC and LHC energies. Here, m_* is taken as 1.05 GeV and the momentum region averaged is 0–1 GeV/c. One can see that the BBC functions decrease with increasing $|\widetilde{y}|$. This is because the average source longitudinal velocity is higher than the average source transverse velocity for hydrodynamic sources with Bjorken longitudinal boost invariance, and the higher longitudinal velocity leads to larger average values of $e^{-k^\mu u_\mu/T_f}$ at $|\widetilde{y}| = 1$ than at $|\widetilde{y}| = 0$ [10,38].

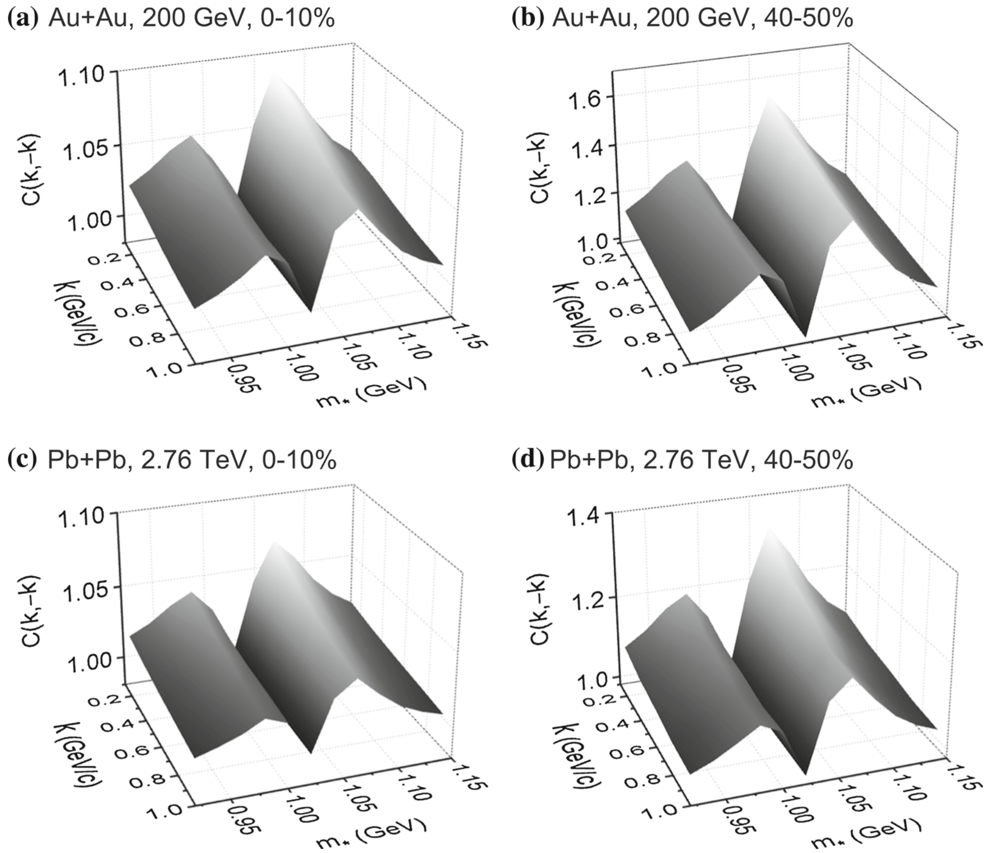

Fig. 4 BBC functions of $\phi\phi$ averaged over event-by-event calculations for 2000 events for central and peripheral collisions of Au + Au at $\sqrt{s_{NN}} = 200$ GeV and Pb + Pb at $\sqrt{s_{NN}} = 2.76$ TeV

4 BBC for Cu + Cu collisions at $\sqrt{s_{NN}} = 200$ GeV

As is well known, the squeezed BBC function is sensitive to the temporal distribution of the particles' freeze-out points. The narrow temporal distribution corresponding to a small hydrodynamic source may lead to a large BBC. We are therefore motivated to investigate next the BBC for heavy-ion collisions of Cu + Cu at $\sqrt{s_{NN}} = 200$ GeV, which have smaller sources compared to those in Au + Au and Pb + Pb collisions.

In Fig. 8a, b, we plot the space-time distributions of the freeze-out points of ϕ meson in the $z = 0$ plane for Cu + Cu collisions at $\sqrt{s_{NN}} = 200$ GeV with impact parameter $b = 0-4$ and 4–8 fm, respectively. The event number for the two impact parameter regions is 2000. One can see that the distributions for Cu + Cu collisions are smaller compared to the distributions in Fig. 1a, b for the Au + Au collisions. In Fig. 9a, b, we show the normalized distributions of time and transverse coordinate of ϕ freeze-out points in the $z = 0$ plane for the Cu + Cu collisions. The normalized time and transverse coordinate distributions are obtained by projecting the space-time distributions in Fig. 8 to the time and transverse coordinate axes, respectively. One can see that the widths of the distributions for peripheral collisions are obviously narrower than those for central collisions.

We plot in Fig. 10a, b the BBC functions of $\phi\phi$ averaged over event-by-event calculations for 2000 events for Cu + Cu collisions with impact parameter $b = 0$–4 and 4–8 fm, respectively. The BBC function for peripheral collisions is larger than that for central collisions. The peaks of the BBC functions reach about 1.3 and 2.5 for central and peripheral collisions, respectively. They are much higher than the corresponding results for Au + Au collisions at the RHIC energy and Pb + Pb collisions at the LHC energy, as shown in Fig. 4. The reason for this is mainly that the temporal distributions for the smaller sources of Cu + Cu collisions are very narrow.

In Fig. 11a, b, we show the dependences of the averaged BBC functions $\phi\phi$, $\langle C(\mathbf{k}, -\mathbf{k})\rangle_{|\mathbf{k}|}$, on the cosine of the particle azimuthal angle ψ and the particle pseudorapidity for Cu + Cu collisions, respectively. Here, m_* is taken as 1.05 GeV and the momentum region averaged is 0–1 GeV/c. One can see that the average BBC functions

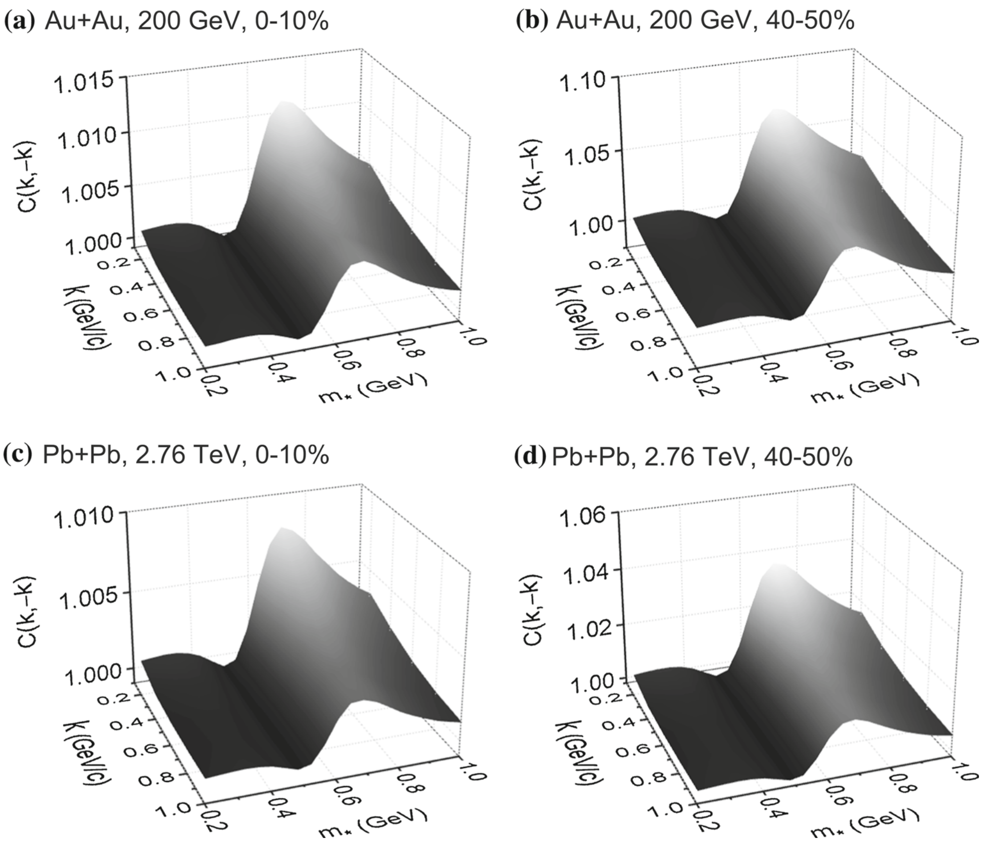

Fig. 5 BBC functions of K^+K^- averaged over event-by-event calculations for 2000 events for central and peripheral collisions of Au + Au at $\sqrt{s_{NN}} = 200$ GeV and Pb + Pb at $\sqrt{s_{NN}} = 2.76$ TeV

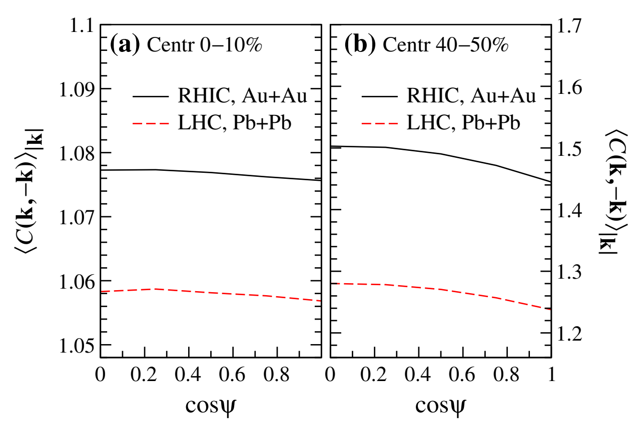

Fig. 6 Dependence of the average BBC functions of $\phi\phi$ on the cosine of the particle azimuthal angle ψ for the collisions at the RHIC and LHC energies. Here, m_* is taken as 1.05 GeV and the momentum region averaged is 0–1 GeV/c

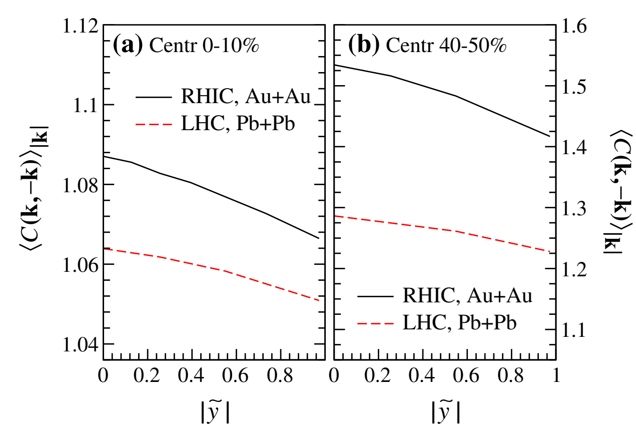

Fig. 7 Dependence of the average BBC functions of $\phi\phi$ on the particle pseudorapidity for the collisions at the RHIC and LHC energies. Here, m_* is taken as 1.05 GeV and the momentum region averaged is 0–1 GeV/c

are almost independent of $\cos\psi$ for central collisions, and they decrease slightly with increasing $\cos\psi$ for peripheral collisions because of the anisotropic transverse expansion [10,38]. As discussed in Sect. 3, the average BBC functions for Cu + Cu collisions also decrease with the increasing $|\widetilde{y}|$ like that for the Au + Au and Pb + Pb collisions.

5 Summary and conclusions

In the hot and dense hadronic sources formed in high-energy heavy-ion collisions, the particle interactions in medium might lead to a squeezed BBC of boson–antiboson pairs. In this paper, we investigate the BBC functions of $\phi\phi$ and

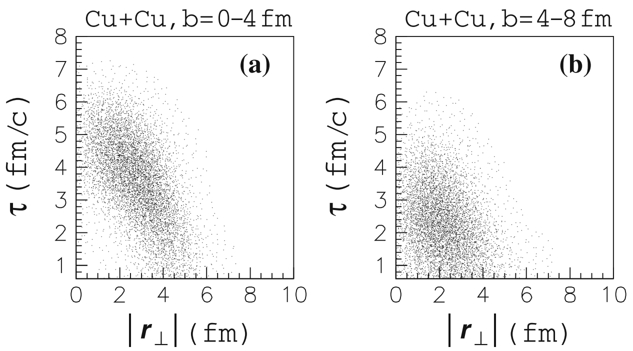

Fig. 8 Distributions of the freeze-out points of ϕ meson in the $z = 0$ plane for Cu + Cu collisions at $\sqrt{s_{NN}} = 200$ GeV and with the impact parameter $b = 0$–4 and 4–8 fm. The number of event is 2000

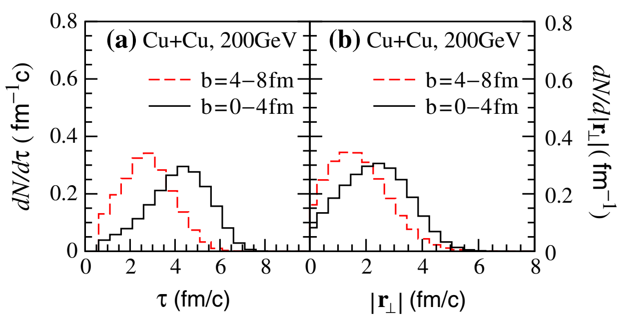

Fig. 9 Normalized distributions of time and transverse coordinate of the ϕ freeze-out points in the $z = 0$ plane for Cu + Cu collisions at $\sqrt{s_{NN}} = 200$ GeV. The *solid lines* are for $b = 0$–4 fm, and the dashed lines are for $b = 4$–8 fm. The number of event is 2000

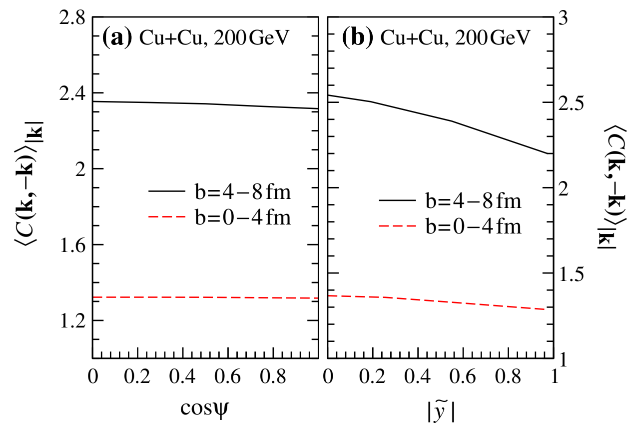

Fig. 11 Dependences of the average BBC functions of $\phi\phi$ on the cosine of the particle azimuthal angle and the particle pseudorapidity for Cu + Cu collisions at $\sqrt{s_{NN}} = 200$ GeV. Here, m_* is taken as 1.05 GeV and the momentum region averaged is 0–1 GeV/c

K^+K^- for heavy-ion collisions of Au + Au at $\sqrt{s_{NN}} = 200$ GeV at the RHIC and Pb + Pb at $\sqrt{s_{NN}} = 2.76$ TeV at the LHC, using (2 + 1)-dimensional hydrodynamics with the FIC generated by HIJING. The investigations indicate that the BBC functions averaged over event-by-event calculations for many events for the hydrodynamic sources with the FIC are smoothed as a function of the particle momentum. This is different from the BBC functions for the hydrodynamic sources with Gaussian initial-energy distributions, which exhibit oscillations with respect to the particle momentum [10]. The BBC functions for collisions of Au + Au at the RHIC energy are larger than those for collisions of Pb + Pb at the LHC energy, because the width of the source's temporal distribution increases with increasing collision energy. The average BBC function, $\langle C(\mathbf{k}, -\mathbf{k})\rangle_{|\mathbf{k}|}$, exhibits a decrease with increasing cosine of the particle azimuthal angle for peripheral collisions because of the anisotropic source transverse velocity. Based on the calculations, we predict that the BBC of $\phi\phi$ may possibly be observed in peripheral collisions of Au + Au at the RHIC energy and Pb + Pb at the LHC energy. The BBC of $\phi\phi$ is large for the smaller sources of Cu + Cu collisions at $\sqrt{s_{NN}} = 200$ GeV. It is of great interest to investigate experimentally the BBC of $\phi\phi$ in high-energy heavy-ion collisions.

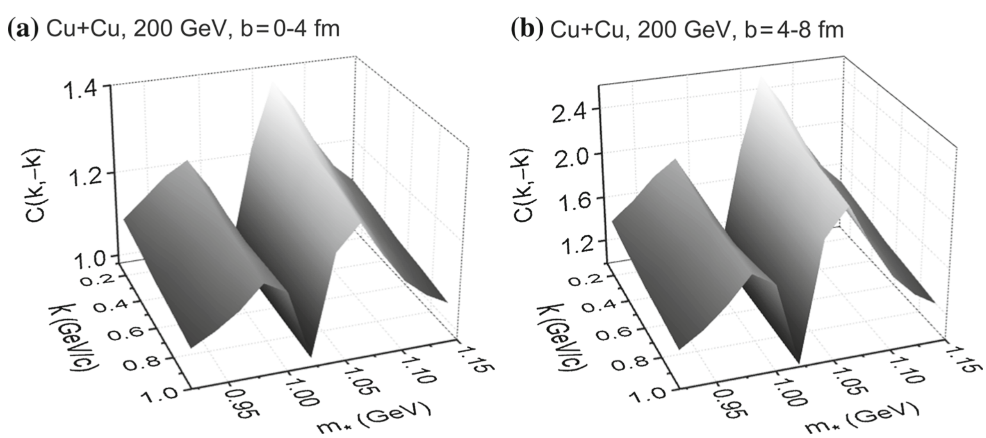

Fig. 10 BBC functions of $\phi\phi$ averaged over event-by-event calculations for 2000 events for Cu + Cu collisions at $\sqrt{s_{NN}} = 200$ GeV and with $b = 0$–4 and 4–8 fm

Acknowledgments This research was supported by the National Natural Science Foundation of China under Grant No. 11275037.

Funded by SCOAP^3.

References

1. M. Asakawa, T. Csörgő, Heavy Ion Phys. **4**, 233 (1996). arXiv:hep-ph/9612331
2. M. Asakawa, T. Csörgő, M. Gyulassy, Phys. Rev. Lett. **83**, 4013 (1999)
3. I.V. Andreev, M. Plümer, R.M. Weiner, Phys. Rev. Lett. **67**, 3475 (1991)
4. I.V. Andreev, M. Plümer, R.M. Weiner, Int. Mod. Phys. A **8**, 4577 (1993)
5. M. Gyulassy, S.K. Kaufmann, L.W. Wilson, Phys. Rev. C **20**, 2267 (1979)
6. A. Makhlin, Yu.M. Sinyukov, Sov. J. Nucl. Phys. **46**, 354 (1987)
7. Yu.M. Sinyukov, Nucl. Phys. A **566**, 589c (1994)
8. S.S. Padula, G. Krein, T. Csörgő, Y. Hama, P.K. Panda, Phys. Rev. C **73**, 044906 (2006)
9. D.M. Dudek, S.S. Padula, Phys. Rev. C **82**, 034905 (2010)
10. Y. Zhang, J. Yang, W.N. Zhang, Phys. Rev. C **92**, 024906 (2015)
11. J. Knoll, Phys. Rev. C **83**, 044914 (2011)
12. X.N. Wang, M. Gyulassy, Phys. Rev. D **44**, 3501 (1991)
13. M. Gyulassy, X.N. Wang, Comput. Phys. Commun. **83**, 307 (1994)
14. C. Shen, U. Heinz, P. Huovinen, H.C. Song, Phys. Rev. C **82**, 054904 (2010)
15. Y. Hu, W.N. Zhang, Y.Y. Ren, J. Phys. G: Nucl. Part. Phys. **42**, 045105 (2015)
16. J.D. Bjorken, Phys. Rev. D **27**, 140 (1983)
17. D.H. Rischke, arXiv:nucl-th/9809044
18. P.F. Kolb, U. Heinz, arXiv:nucl-th/0305084
19. G. Baym, B.L. Friman, J.P. Blaizot, M. Soyeur, W. Czyż, Nucl. Phys. A **407**, 397 (1983)
20. M. Gyulassy, D.H. Rischke, B. Zhang, Nucl. Phys. A **613**, 397 (1997)
21. Z.W. Lin, C.M. Ko, B.A. Li, B. Zhang, S. Pal, Phys. Rev. C **72**, 064901 (2005)
22. L.G. Pang, Q. Wang, X.N. Wang, Phys. Rev. C **86**, 024911 (2012)
23. A. Harten, P.D. Lax, B. van Leer, SIAM Rev. **25**, 35 (1983)
24. B. Einfeldt, SIAM J. Numer. Anal. **25**, 294 (1988)
25. V. Schneider, U. Katscher, D.H. Rischke et al., J. Comput. Phys. **105**, 92 (1993)
26. D.H. Rischke, S. Bernard, J.A. Maruhn, Nucl. Phys. A **595**, 346 (1995)
27. D.H. Rischke, M. Gyulassy, Nucl. Phys. A **608**, 479 (1996)
28. G.A. Sod, J. Fluid Mech. **83**, 785 (1977)
29. W.N. Zhang, M.J. Efaaf, C.Y. Wong, M. Khaliliasr, Chin. Phys. Lett. **10**, 1918 (2004)
30. M.J. Efaaf, W.N. Zhang, M. Khaliliasr et al., High Energy Phys. Nucl. Phys. **29**, 46 (2005)
31. M.J. Efaaf, W.N. Zhang, M. Khaliliasr et al., High Energy Phys. Nucl. Phys. **29**, 467 (2005)
32. W.N. Zhang, M.J. Efaaf, C.Y. Wong, Phys. Rev. C **70**, 024903 (2004)
33. L.L. Yu, W.N. Zhang, C.Y. Wong, Phys. Rev. C **78**, 014908 (2008)
34. H.J. Yin, J. Yang, W.N. Zhang, L.L. Yu, Phys. Rev. C **86**, 024914 (2012)
35. P.F. Kolb, J. Sollfrank, U. Heinz, Phys. Rev. C **62**, 054909 (2000)
36. P.F. Kolb, R. Rapp, Phys. Rev. C **67**, 044903 (2003)
37. J. Adams et al. (STAR Collaboration), Phys. Rev. C **72**, 014904 (2005)
38. Y. Zhang, J. Yang, W.N. Zhang, Int. J. Mod. Phys. E **24**, 1550071 (2015)